

Design of 100kW Brushless DC Motor for Advanced Actuation System using Comsol

Shinoy K S

Scientist

CEAG/AVN/VSSC

Thiruvanthapuram

Baby Sebastian

DH, SDCD

VSSC

Thiruvanthapuram

M N Namboodiripad

GD, CEAG

VSSC

Thiruvanthapuram

Abstract: This paper presents the design and analysis of a high power radial flux Brushless DC motor for electro mechanical actuation system. The motor is used for driving an electro mechanical actuator of 20 ton capacity. Surface mounted, radially magnetized permanent magnet design is mostly preferred due to its ease of control, high efficiency and low maintenance. The motor under consideration is having four set of windings and four set of sensors for redundancy. The motor is rated for a maximum torque of 133Nm (@95A) per winding and a total torque of 532 Nm (@380 A) when all the windings are excited. The speed of the motor is 1850 rpm at a nominal voltage of 270V. The performance evaluation of radially magnetized permanent magnet motors for a three phase, 108 slots, 24 pole BLDC motor was carried out in finite element analysis software COMSOL. The number of poles has been chosen such that the motor mechanical envelop has been met and has high efficiency.

Keywords: Surface mounted, radially magnetized, cogging torque, redundancy

NOMENCLATURE

B	= Magnetic flux density (T)
B_g	= Magnetic flux density at the air gap (T)
K_b	= Back EMF constant
K_t	= Torque constant
n	= Speed of rotation (rpm)
I	= current amplitude (A)
L	= active motor length
D_r	= rotor outer diameter
N_{ph}	= Number of phases
$N_{ph} - 1$	= Number of phases conducting simultaneously.
N_t	= number of turns per phase
K_w	= winding factor
α	= pole-arc coefficient
D_r	= Outer diameter of the motor
L_{eq}	= Inductance of the stator winding (H)
H	= Magnetic intensity

I. INTRODUCTION

PERMANENT magnet (PM) brushless DC motors have been widely used because of their attractive features like compactness, low weight, high efficiency, and ease in control [1]. The reliability of BLDC motor is high since it does not have any brushes to wear out and replace. The stator consists of stacked steel laminations with windings placed in the slots where as the rotor is made of permanent magnet that can vary from two to twelve pole pairs with alternate north and south poles.

Different rotor configurations are available for PMBLDC motor namely surface mounted PM design with interior or exterior rotor, interior PM design with buried magnets etc., each having specific strengths and weaknesses. Among these the radial-flux, surface mounted type is commonly used for its simplicity for manufacturing and assembling. But this type of motors provides low inductance value so that the overall time constant is reduced. The motor used in servo application should have low cogging torque, high efficiency, fault tolerant and should be compact in dimension.

Finite Element (FEM) analysis using COMSOL software is done for this motor configuration. The simulation results are presented in the section III.

II. PM BLDC MOTOR DESIGN AND ANALYSIS

The analysis is being carried out for a three phase motor having 108 slots and 24 permanent magnets. Samarium-Cobalt (Sm₂Co₁₇) is the magnet material used due to its high residual flux density, energy density and good thermal stability allowing its use in applications exposed to high temperature. The specifications of the motor used for the analysis are listed in table I.

TABLE I. MOTOR SPECIFICATIONS

Winding	Quadruplex winding
Hall sensor	Four sets
Peak torque	133 Nm
Supply voltage	270 V
Torque constant K_t	1.4 Nm/A +/- 10%
Back emf constant K_b	1.4 V/rad/sec +/- 10%
No load speed	1850 rpm
Cogging torque	1 Nm

Table II. Major Dimensional Specifications of Three phase Motor

Outer diameter of stator	195 mm
Inner diameter of stator	131.2 mm
Inner diameter of rotor	100 mm
Total length of stator	226 mm
Length of stack	200 mm
Length of rotor	210 mm
Overhang (lead side)	15 mm
Overhang(non lead side)	11 mm

Table 2 shows the major dimensional specification required in order to accommodate the motor inside the electromechanical actuator. Owing to the symmetry in the configuration, a quadrant of the motor is considered. Since there are 108 slots per 12 pole pairs, it can be analyzed as 9 slots per a pole pair. Being a three phase motor, each winding are electrically separated by 120°. Each slot is displaced 40 electrical degrees apart. The winding diagram for this motor with the given specifications is shown in table 3. The finite element method is used for analysis. COMSOL provides finite element analysis by meshing the whole assembly, so that the calculated or predicted result gets closer to the actual values with increasing mesh density, provided that the boundary conditions and other parameters have been correctly modeled [6]. The meshed plot of the high power motor is shown in fig.1.

Phases	1	2	3	4	5	6	7	8	9
Electrical angle	0	40	80	120	160	200	240	280	320
R	R	R				R			
Y			B'				B	B	
B				Y	Y				Y'

TABLE III. WINDING DIAGRAM OF 108 SLOT 24 POLE MOTOR

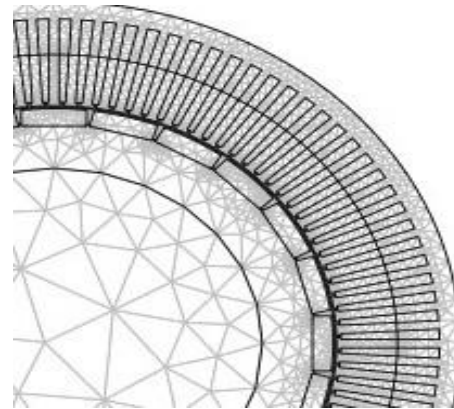


Fig.1a. Mesh generated for a quadrant

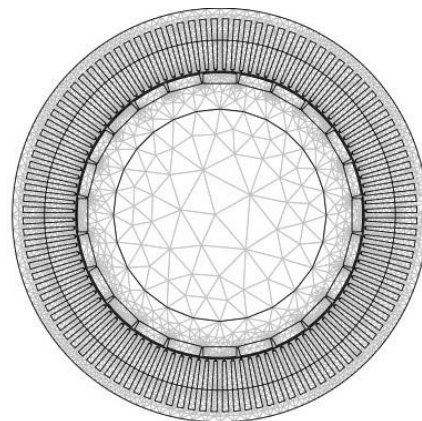


Fig.1b. Mesh generated for full motor

The magnetic flux density is calculated from the magnetic vector potential, A [7] and can be expressed as in equation 1.

$$\mathbf{B} = \mu_0 \mu_r \mathbf{H} = \nabla \times \mathbf{A} \quad (1)$$

Where μ_0 is the permeability of free space and μ_r is the permeability of the material. The detailed configurations are presented in the following sections.

DESIGN OF THREE PHASE BLDC MOTOR

The required technical specifications and dimensional constraints are given in table 1 and table 2 respectively. Initially the magnetic circuit is designed based on equations given in [12] from which the airgap flux density can be calculated. Making a compromise between the switching frequency and back iron depth the number of poles is fixed at 24. As the designed motor should possess minimum cogging torque, slot number is fixed as 108 utilizing the advantage of fractional slot winding. The width of back iron is calculated based on the flux present in the machine as per equations in [13].

Turns per phase can be calculated from design equations as given in [12]-[13]. The equation for back emf is given in equation (1)

$$\text{Back emf } e_b = (m-1)N_{ph}K_w L D_i \alpha B_g \omega = K_b \omega \quad (1)$$

Where K_b is the back emf constant, m is the number of phases, L is the active motor length, K_w is the winding factor, α is the pole arc coefficient, D_i is the stator inner diameter, N_{ph} is the turns per phase, B_g is the airgap flux density, ω is the speed of the motor in rad/sec.

The equation for torque is given in equation (2)

$$\text{Torque } T_e = (m-1)N_{ph}K_w L D_i \alpha B_g i = K_t i \quad (2)$$

where i is the current, K_t is the torque constant.

(1), (2) are solved for three phase motor. The turns per phase for three phase motor is obtained as 45. The designed values are summarized in table 4.

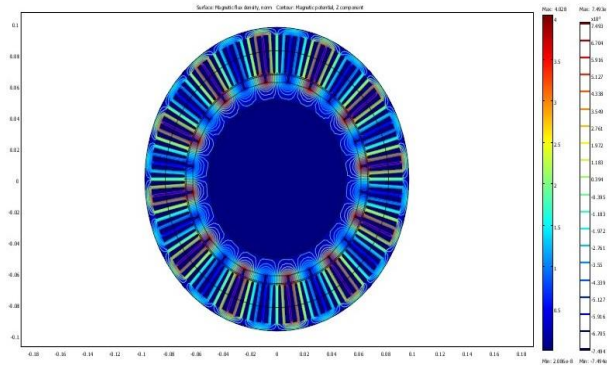


Fig.2. Magnetic flux distribution plot & flux contours

TABLE IV DESIGNED VALUES

Number of slots	180
Number of poles	24
Width of magnet	5 mm
Airgap length	1 mm
Airgap flux density	0.8 T

The cosine and sine angles for SMPM are given by the expressions 3 and 4.

$$\cos \theta = \frac{B * x}{\sqrt{x^2 + y^2}} \quad (3)$$

$$\sin \theta = \frac{B * y}{\sqrt{x^2 + y^2}} \quad (4)$$

III SIMULATION USING COMSOL SOFTWARE

The simulation is basically the numerical solution of magnetic vector potential in different sub domains of the motor. Once magnetic vector potential is found remaining parameters like flux density, induced emf are found using Maxwell's equations. Torque is computed using the stress tensor technique

Magnetic flux density variation at the air gap

Fig.3 shows the magnetic flux density variation at the air gap. The BLDC motor is having an average value of almost 0.8T. The result obtained is for the magnet size taken into consideration. The magnet height when increased could increase the flux density, but it also affects other parameters like cogging torque, saturation of core etc.

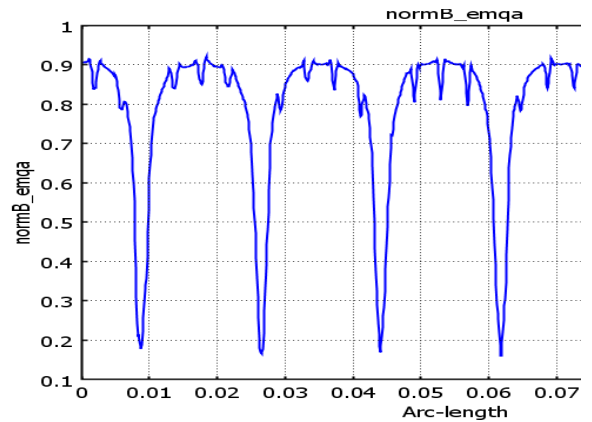


Fig.3. B_g Air gap flux density plot

A. Difference in Inductance calculated.

Using COMSOL inductance value could be calculated in two ways namely: Energy method and virtual work method. In energy method the magnetic energy density, W is obtained from the sub-domain integration using the expression of energy density. Then the inductance (L_{eq}) can be calculated using the equation given by equation 6. Here the current is usually taken in the milli ampere range.

$$W = \frac{1}{2} L_{eq} I^2 \quad (5)$$

Using the other method (Method of virtual work) the analysis is done in time dependent transient mode. The currents in the stator windings are expressed as either the function of sine and cosine terms (Eg. $J_R = N * I_m \sin(\omega * t) / A$). After solving, the induced voltage is plotted to obtain the inductance value using Ohms Law.

$$L_{eq} = \frac{V(\text{induced})}{I^2} \quad (6)$$

In both these cases permanent magnet flux density is kept zero to avoid the flux variation due to magnets. The table 3 shows the calculated inductances for the both configuration.

TABLE V. COMPARISON OF INDUCTANCES WITH EXPERIMENTAL RESULTS

Method Employed	With 2 phases excited (mH)	With R phase excited (mH)	Experimental Results (mH)
Using Energy Method	7.5	2.3	7.8
Using Virtual work method	7.6	2.37	7.8

The electromotive force (EMF), E contributing to the electromagnetic power is:

$$E = (N_{ph} - 1)2\pi N_t K_w \alpha D_r L B_g n = K_b n \quad (7)$$

The generated voltage is computed as the line integral of the electric field, E_z along the winding. i.e. it is obtained by taking the average z component of electric field for each winding cross section and multiplying it by the axial length of the rotor, and taking sum over all winding cross sections[7].

$$E = N \sum \frac{L}{A} \int E_z dA \quad (8)$$

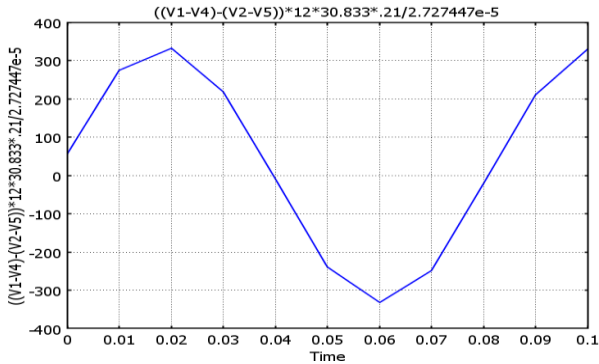


Fig.4. Back EMF plot at rated speed

The general equation for electromagnetic torque, T is:

$$T = (N_{ph} - 1)N_t K_w \alpha D_r L B_g i = K_t i \quad (9)$$

The torque plot when two phases are excited with constant dc current is shown in fig.5. Here the length of the motor is taken 210 mm ie the reason why a multiplication of 0.21 comes in torque computation. The torque is computed in COMSOL using the Maxwell's stress tensor method.

$$T = \oint_B (r - r_o) \times (n_1 T_2) dS \quad (10)$$

Where r_0 is the point on the axis of rotation and n is unit vector normal to the surface S.

T_2 is Maxwell stress tensor

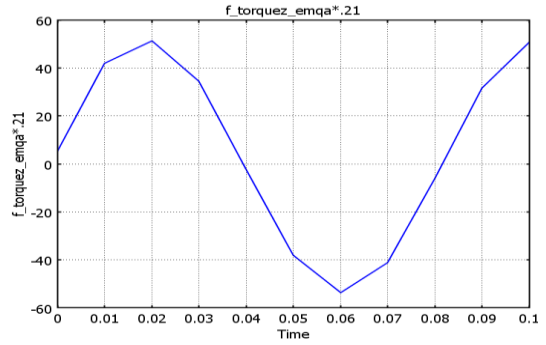


Fig.5.Torque produced with 2 phases excited

Cogging torque as mentioned before is one of the major concern of PM motors. As fractional slot pitch winding is used, considerable reduction in cogging torque is achieved. The cogging torque profile for the motor have been plotted as seen in fig. which varies from -0.5Nm to -3Nm in SMPM . This can vary with the dimensions that we choose. With these specifications listed above cogging torque profile should have 216 cycles in a second, which is the LCM of number of slots and poles.

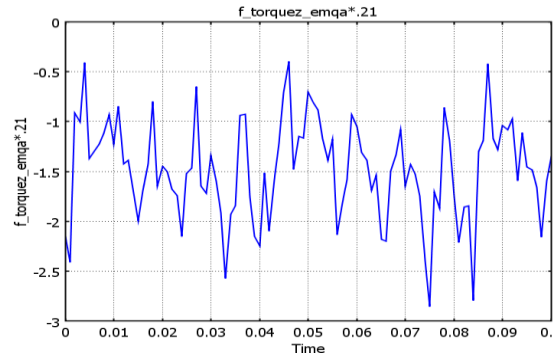


Fig.6.Cogging torque variation for SMPM motor

V. CONCLUSION

A variety of rotor configurations are possible for a permanent magnet BLDC motor. This paper presents a radially magnetized surface mounted PM motor having 108 slots, 24 poles, three phase motor for a 20 ton electromechanical actuator. SMPM motor offers more air gap flux density when compared to any other configuration. The motor used for the analysis provides fractional slot design so that the cogging torque was found to be only 0.89 % of the full load torque which is considerably low. This COMSOL finite element software has been used for

analyzing and for optimising the design requirements. Computation of inductance value by analytical method is difficult but finite element simulation gives correct value which is an important parameter in motor design. Other parameters like cogging torque, saturation etc can be studied by using comsol software. The motor has been realized and is under the process of testing.

REFERENCES

- [1] L. Parsa, "On advantages of multiphase machines", 31st Annual Conference of Industrial Electronics 2005, IECON 2005
- [2] Praveen R.P., Ravichandran M.H., V. T. Sadasivan Achari, Jagathy Raj V. P., G. Madhu, and G.R. Bindu, "Design and Analysis of Zero Cogging Brushless DC Motor for Spacecraft Applications", ECTI Transactions On Electrical Eng., Electronics, And Communications Vol.9, No.1 February 2011
- [3] Sang-Moon Hwang, Jae-Boo Eom, Geun-Bae Hwang, Weui-Bong Jeong, and Yoong-Ho Jung, "Cogging Torque and Acoustic Noise Reduction in Permanent Magnet Motors by Teeth Pairing", IEEE Transactions On Magnetics, Vol. 36, No. 5, September 2000
- [4] Guowei Zhang, Fengxiang Wang, Yongshan Shen, "Reduction of Rotor Loss and Cogging Torque of High Speed PM Machine by Stator Teeth Notching, Proceeding of International Conference on Electrical Machines and Systems 2007, Oct. 8-11, Seoul, Korea
- [5] Jin Wang, Libing Zhou, Tong Yang and Yue Wang, "Cogging Torque Reduction in Interior Permanent Magnet Brushless DC Motor with Flux-Concentration Type Rotor"
- [6] Teeradej Srisiriwanna, Mongkol Konghirun, A Study of Cogging Torque Reduction Methods in Brushless DC Motor
- [7] Shailesh Waikar Til & Gopalathnam Hamid A Toliyat Julio C. Moreira, Evaluation Of Multiphase Brushless Permanent Magnet (BPM) Motors Using Finite Element Method (FEM) and Experiments
- [8] M. Godoy Simões, N. N. Franceschetti, P. Vieira Jr Design and Evaluation of a Polyphase Brushless DC Machine Direct Drive System
- [9] Yuqi Rang, Hao Xiong, Qiang Wu Guangwei Meng, Huaishu Li, Libing Zhou, FEM Simulation and Harmonic Torque Analysis of Six-Phase BLDC Motor
- [10] Frank Scullier, "Magnet Shape Optimization to Reduce Pulsating Torque for a Five-Phase Permanent-Magnet Low-Speed Machine", IEEE Transactions on Magnetics, vol. 50, no. 4, April 2014
- [11] Kiran George, Sija Gopinathan, Shinoy K.S., A Comparison of Three Phase and Five Phase BLDC Motor, International Journal of Advanced Research in Electrical, Electronics and Instrumentation Engineering, Vol. 2, Special Issue 1, December 2013.
- [12] Duane C. Hanselman, Brushless Permanent Magnet Motor Design", Second Edition 2006
- [13] J. R. Hendershot Jr And TJE Miller, "Design of brushless permanent-magnet motors", 1994
- [14] Why do infinite Element Analysis-NAFEMS
- [15] COMSOL3.5a manual
- [16] J.R.Hendershot Jr., T.J.E. Miller. Design of brushless Permanent magnet motors. Magna Physics publishing and Clarendon press-Oxford 1994.
- [17] P. Ji, W. Song, and Y. Yang, "Overview on application of permanent magnet brushless DC motor," Electrical Machinery Technology, vol.40, pp.32-36, Feb. 2003.
- [18] P. Pillay, R. Krishnan, Modeling, Simulation and Analysis of Permanent-Magnet Motor Drives, Part II: The Brushless DC Motor Drive, IEEE Trans. on Industry Applications, March/April, 1989, pp.274-279.
- [19] F. Libert, J. Soulard, "Design study of different Direct-Driven Permanent-Magnet Motors for a low Speed Application", Division of Electrical Machines and Power Electronics, Sweden.
- [20] Guangwei Meng, Hao Xiong, Huaishu Li, "FEM Analysis and simulation of Multi-phase BLDC Motor" Naval University of Engineering, Wuhan, China